Bioorganic & Medicinal Chemistry Letters 21 (2011) 2564–2567

Contents lists available at ScienceDirect

Bioorganic & Medicinal Chemistry Letters

journal homepage: www.elsevier.com/locate/bmcl

Probing the inhibitor selectivity pocket of human 20α-hydroxysteroid dehydrogenase (AKR1C1) with X-ray crystallography and site-directed mutagenesis

Ossama El-Kabbani [a,*], Urmi Dhagat [a], Midori Soda [b], Satoshi Endo [b], Toshiyuki Matsunaga [b], Akira Hara [b]

[a] Medicinal Chemistry and Drug Action, Monash Institute of Pharmaceutical Sciences, Monash University, 381 Royal Parade, Parkville, Victoria 3052, Australia
[b] Laboratory of Biochemistry, Gifu Pharmaceutical University, Daigaku-Nishi, Gifu 501-1196, Japan

ARTICLE INFO

Article history:
Received 25 December 2010
Revised 17 January 2011
Accepted 19 January 2011
Available online 22 January 2011

Keywords:
Aldo-keto reductase
3-Chloro-5-phenylsalicylic acid
Cancer
Drug design
Human 20α-hydroxysteroid dehydrogenase

ABSTRACT

Human 20α-hydroxysteroid dehydrogenase (AKR1C1) is an important drug target due to its role in the development of lung and endometrial cancers, premature birth and neuronal disorders. We report the crystal structure of AKR1C1 complexed with the first structure-based designed inhibitor 3-chloro-5-phenylsalicylic acid (K_i = 0.86 nM) bound in the active site. The binding of 3-chloro-5-phenylsalicylic acid to AKR1C1 resulted in a conformational change in the side chain of Phe311 to accommodate the bulky phenyl ring substituent at the 5-position of the inhibitor. The contributions of the nonconserved residues Leu54, Leu306, Leu308 and Phe311 to the binding were further investigated by site-directed mutagenesis, and the effects of the mutations on the K_i value were determined. The Leu54Val and Leu306Ala mutations resulted in 6- and 81-fold increases, respectively, in K_i values compared to the wild-type enzyme, while the remaining mutations had little or no effects.

The aldo-keto reductase (AKR) superfamily comprises a group of structurally related NAD(P)(H)-dependent proteins that catalyse the oxidation and reduction of a variety of endogenous and xenobiotic compounds. These enzymes are made up of a TIM-barrel (triose phosphate isomerase) motif consisting of an eight-stranded β-sheet surrounded by eight α-helices.[1] There are four human AKRs which belong to the AKR1C subfamily of this superfamily. These four AKR1C isoforms, namely, AKR1C1, AKR1C2, AKR1C3 and AKR1C4 are known as 20α-hydroxysteroid dehydrogenase (HSD), type 3 3α-HSD, type 2 3α-HSD and type 1 3α-HSD, respectively, due to their roles in catalysing oxidation and reduction of steroidal compounds.[2,3] Although these enzymes are highly homologous, with greater than 80% sequence homology, they have different physiological roles and exhibit distinct positional and stereo preferences with respect to their substrates.[4] The functional plasticity of the AKR1C isoforms highlights their ability to modulate levels of active steroid hormones such as androgens, estrogens and progestins at the pre-receptor level.[5]

AKR1C1 is a progesterone metabolising enzyme which plays an important role in endometrial development, maintenance of pregnancy and neuronal function by controlling the cellular concentration of progesterone.[6,7] AKR1C1 also plays an important role in brain function where it regulates the occupancy γ-aminobutyric acid type A ($GABA_A$) receptors by reducing neuroactive steroids such as (3α,5α-tetrahydroprogesterone and 5α-tetrahydrodeoxycorticosterone) to inactive 20α-hydroxysteroids thereby removing them from the synthetic pathway.[8] On the other hand, expression of AKR1C1 is elevated in human cancers in the lung, endometrium, ovary and skin,[9–12] and a recent report shows fibrosarcoma formation in nude mice by subcutaneous injection of NIH3T3L1 cells expressing AKR1C1.[13] It is also suggested that overexpression of AKR1C1 is related to drug-resistance against some anti-cancer agents.[12,14–16] Thus, there is a growing need for the discovery and design of specific inhibitors for AKR1C1 which could be used for the development of new improved therapeutic agents for premature birth, neuronal disorders and cancer therapy.

AKR1C1 is inhibited both non-competitively by benzodiazepines, pyrimidine and anthranilic derivatives and competitively by *N*-phenylanthranilic acid derivatives, steroid carboxylates and flavones.[17–19] Moreover, our laboratory has demonstrated that AKR1C1 is potently inhibited by salicylic acid derivatives, of which the rationally designed 3-chloro-5-phenylsalicylic acid (CPSA) is the most potent competitive inhibitor showing a K_i value of 0.86 nM.[20–23] In order to characterize the detailed structural

Abbreviations: HSD, hydroxysteroid dehydrogenase; AKR, aldo-keto reductase; AKR1C1, human 20α-hydroxysteroid dehydrogenase; *S*-Tetralol, *S*-(+)-1,2,3,4-tetrahydro-1-naphthol; $GABA_A$, γ-aminobutyric acid type A; CPSA, 3-chloro-5-phenylsalicylic acid; DCSA, 3,5-dichlorosalicylic acid; WT, wild-type.

* Corresponding author. Tel.: +61 3 9903 9691; fax: +61 3 9903 9143.
E-mail address: ossama.el-kabbani@monash.au (O. El-Kabbani).

0960-894X/$ - see front matter © 2011 Published by Elsevier Ltd.
doi:10.1016/j.bmcl.2011.01.076

interactions between CPSA and AKR1C1, the crystal structure of the enzyme–inhibitor complex was determined at a resolution of 1.87 Å and the roles of the amino acid residues lining the selectivity pocket in inhibitor binding were further investigated by site-directed mutagenesis. The results may facilitate further development of AKR1C1 inhibitors that may be used as anticancer agents.

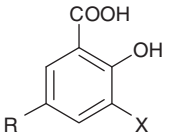

Scheme 1. 3,5-Disubstituted salicylic acids. CPSA: X = Cl, R = phenyl; DCSA: X = R = Cl.

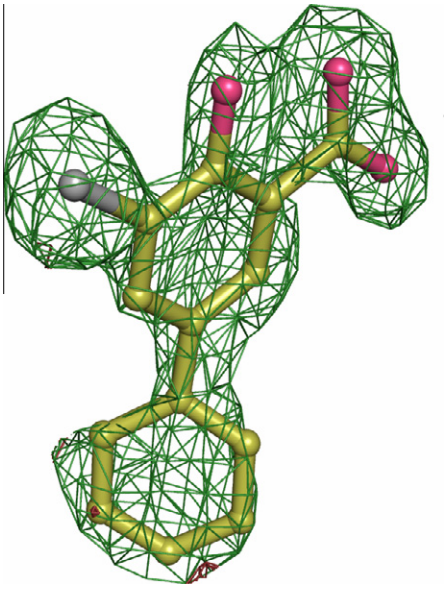

Figure 1. The inhibitor CPSA superimposed on the corresponding $F_o - F_c$ electron density map calculated with the inhibitor excluded from the model at 1.87 Å resolution and contoured at a 3σ cut-off. The carbon, oxygen and chloride atoms are shown in green, red and grey colours, respectively.

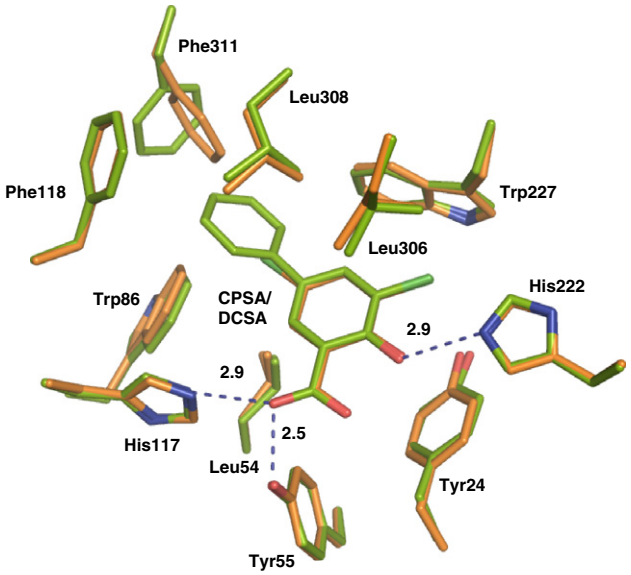

Figure 2. Superimposition of the crystal structures of AKR1C1 with bound DCSA (shown in orange) and CPSA (shown in green). Hydrogen bond interactions between CPSA and the catalytic residues are shown as dotted lines with corresponding distances given in angstroms.

Crystals of AKR1C1 in ternary complex with $NADP^+$ and the inhibitor CPSA (Scheme 1) were obtained after optimisation of the crystallization conditions previously described.[21] Crystals diffracted to a maximum resolution of 1.87 Å with one monomer per asymmetric unit and an estimated 35.9% solvent content. The refined model with final R_{cryst} = 18.5% and R_{free} = 25.0% consisted of 318 amino acid residues, missing the first six N-terminal residues due to lack of corresponding electron density, 379 solvent molecules, one $NADP^+$ molecule, one inhibitor molecule and a zinc ion from the crystallisation buffer. The backbone dihedral angles of 92.6% and 7.1% of the residues were in the most favoured and allowed regions, respectively, in the Ramachandran plot. As observed previously in published crystal structures of AKR1C1 only Ser221 was in the disallowed region due to the hydrogen bond between its main-chain and the cofactor molecule.[21,23] A summary of the refinement statistics of the final model is provided in Table 1.

Like all members of the AKR superfamily, AKR1C1 has an $(\alpha/\beta)_8$ TIM-barrel structural motif with $NADP^+$ bound adjacent to an active site located at the C-terminal end of the barrel. The inhibitor, CPSA, was bound in the active site in an orientation similar to that of 3,5-dichlorosalicylic acid (DCSA),[21] with its hydroxyl group pointing towards His222 and the phenyl group extending into a hydrophobic pocket. Clear electron density allowed unambiguous

Table 1
X-ray data collection and refinement statistics

Data collection and processing	
Space group	$P2_1$
Cell dimensions	a = 39.60 Å
	b = 84.05 Å
	c = 49.05 Å
	β = 91.41°
Radiation source	Rotating anode
Wavelength (Å)	1.54178
Diffraction data[a]	
Resolution (Å)	30–1.87 (1.93–1.87)
No. of observed unique reflections	22,148 (1852)
No. of possible unique reflections	24,636 (2283)
Redundancy	3.3 (3.2)
Completeness (%)	89.9 (81.1)
I/σ (I)	7.5 (1.7)
R_{merge} (%)	9.1 (35.2)
Refinement statistics	
Resolution (Å)	30–1.87
Protein residues	318
Solvent molecules	379
Zinc ion	1
Cofactor	1
Inhibitor	1
R_{free} (%)	25.0
R_{cryst} (%)	18.5
RMSDs	
Bonds (Å)	0.022
Angles (°)	1.85
Ramachandran plot	
Residues in most favored regions (%)	92.6
Residues in allowed regions (%)	7.1
Estimated coordinated error	
Luzzati mean coordinate error (Å)	0.240
Mean B factors (Å^2)	
Protein	24.2
$NADP^+$	19.3
Inhibitor	19.1
Zinc ion	23.8
Waters	36.0

[a] Statistics for the highest resolution shell (1.93–1.87 Å) are shown in parentheses.

Table 2
Alteration of K_i values for CPSA and DCSA by site-directed mutagenesis of AKR1C1

Inhibitor	K_i value[a] (nM)						
	WT	Leu54Val	Leu306Ala	Leu308Val	Leu308Ala	Phe311Leu	Phe311Ala
CPSA	0.86 ± 0.01[c]	4.8 ± 0.4 (6)	70 ± 3 (81)	1.7 ± 0.1 (2)	1.2 ± 0.1 (1)	0.85 ± 0.1 (1)	1.5 ± 0.2 (2)
DCSA	5.9 ± 0.8[b]	85 ± 7.6[b] (14)	273 ± 29[b] (46)	78 ± 9[c] (13)	2790 ± 300[b] (473)	7.0 ± 1.0 (1)	6.6 ± 0.2 (1)

[a] The number of folds increase in K_i value relative to that of WT is shown within parenthesis.
[b] From Dhagat et al.[21]
[c] From El-Kabbani et al.[23]

fitting of CPSA in the difference Fourier map ($F_o - F_c$) shown in Figure 1. The torsion angle between the two phenyl rings of CPSA is equal to 33.9°. The carboxylate group of the inhibitor molecule forms hydrogen bonds with the catalytic residues His117 (2.9 Å) and Tyr55 (2.5 Å), while the hydroxyl group is hydrogen bonded to His222 (2.9 Å). The inhibitor makes van der Waals contacts with side chains of Trp86, Phe118, Leu306, Leu308, Phe311 and Trp227. The interactions between the inhibitor and the active site residues are shown in comparison to the structure of AKR1C1 with bound DCSA in Figure 2.

Our earlier structural and kinetic studies suggested that the interactions between the salicylic acid-based inhibitors and the four nonconserved amino acid residues at positions 54, 306, 308 and 311 confer inhibitor selectivity for the four AKR1C isoforms.[21,22] CPSA was designed with its phenyl group targeting a nonconserved hydrophobic pocket in the active site of AKR1C1 lined by residues Leu54, Leu308 and Phe311, resulting in a 24-fold improved potency (K_i = 0.86 nM) over the structurally similar AKR1C2.[23] A comparison between the crystal structures of AKR1C1 with bound DCSA and CPSA revealed that a conformational change in the side chain of Phe311 occurred in the presence of CPSA to accommodate the bulky phenyl ring substituent at the 5-position of the inhibitor (Scheme 1). The contributions of the nonconserved residues Leu54, Leu306, Leu308 and Phe311 to CPSA binding were further investigated by mutations to valine and alanine or leucine (for Phe311) residues, and determining the effects of the mutations on the inhibition constants (K_i values), which imply the dissociation constants of CPSA because of its competitive inhibition with respect to the substrate *S*-(+)-1,2,3,4-tetrahydro-1-naphthol (*S*-tetralol). The Leu54Val and Leu306Ala mutations resulted in increases of 6- and 81-fold, respectively, in the K_i value compared to that of the wild-type enzyme (WT), while the remaining mutations had no or little effects on this value (Table 2).

The above results suggest that van der Waals contacts (Table 3) formed by the bulky side-chains of Leu54 and Leu306 play an important role in the binding of CPSA to AKR1C1, as evidenced by the effects of shortening their side-chains to Val and Ala, respectively, on the K_i value (Table 2). The effects resulting from the Leu308 mutations on the K_i value for DCSA (missing the phenyl moiety of CPSA at the 5-position) were greater than that for CPSA. This may be due to additional van der Waals contacts occurring between the side-chain of Phe311 and the phenyl ring of CPSA in the mutant enzymes missing the bulky Leu308 side-chain (Leu308Val/Leu308Ala) which contributes to inhibitor potency. On the other hand, the effects resulting from the Phe311 mutations on the K_i values for CPSA and DCSA (Table 2) were similar and may be attributed to the conformational change in the side-chain of Phe311 (Fig. 2), in addition to van der Waals contacts formed between the side-chain of Leu308 and the phenyl ring of CPSA (Table 3). It is worth mentioning that in an earlier study we have shown that a conformational change that accompanied the binding of the aldose reductase inhibitor tolrestat to aldehyde reductase, a member of the AKR superfamily, resulted in a reduction of inhibitor potency.[24]

Table 3
Number of van der Waals contacts (<4 Å) between side-chains of Leu54, Leu306, Leu308 and Phe311 in AKR1C1 and the 3-chlorosalicylic (CPSA and DCSA), 5-phenyl (CPSA) and 5-chloro (DCSA) moieties of the inhibitors

Inhibitor moiety	Amino acid side-chain			
	Leu54	Leu306	Leu308	Phe311
3-Chlorosalicylic	2	3	2	–
5-Phenyl	1	–	8	2
5-Chloro	1	–	1	–

In summary, the crystal structure of AKR1C1 in complex with the first structure-based designed inhibitor was determined at 1.87 Å resolution. The inhibitor is bound in the active site with its phenyl moiety at the 5-position occupying a hydrophobic selectivity pocket lined by Leu54, Leu308 and Phe311. Moreover, a comparison of the AKR1C1 crystal structures with bound CPSA and DCSA revealed that a conformational change occurred in the side chain of Phe311 upon CPSA binding to accommodate the bulky phenyl ring of the inhibitor. The effects of replacing the nonconserved Leu54, Leu306, Leu308 and Phe311 with less bulky residues (Val, Ala and Leu) on the K_i values were determined. While the Leu54Val and Leu306Ala mutations resulted in 6- and 81-fold increases in K_i values, respectively, the remaining mutations had no effect suggesting that van der Waals contacts formed by the bulky side-chains of Leu54 and Leu306 play a significant role in the binding of CPSA to AKR1C1. Furthermore, the replacement of the electronegative Cl atom at the 5-position of DCSA with the bulky phenyl moiety in CPSA improved potency suggesting that van der Waals interactions with AKR1C1 and not the electron-withdrawing effect of the substituent at the 5-position is a requisite for potent inhibition.

Atomic coordinates of AKR1C1–CPSA have been deposited in the Protein Data Bank (ID code 3NTY) and will be immediately released upon publication.

Acknowledgements

We thank Tom Day and Peter Scammells for providing CPSA for crystallization. U.D. is a recipient of Monash Graduate School postgraduate scholarship. This work was supported in part by grants for young scientists and scientific research from the Japan Society for the Promotion of Science (to S.E. and A.H.).

Supplementary data

Experimental procedures including site-directed mutagenesis and purification of recombinant enzymes, assay of enzyme activity, crystallization and X-ray data collection and structural determination will be available free of charge via the Internet. Supplementary data associated with this article can be found, in the online version, at doi:10.1016/j.bmcl.2011.01.076.

References and notes

1. Jez, J. M.; Bennett, M. J.; Schlegel, B. P.; Lewis, M.; Penning, T. M. *Biochem. J.* **1997**, *326*, 625.
2. Penning, T. M. *Endocr. Rev.* **1997**, *18*, 281.
3. Mindnich, R. D.; Penning, T. M. *Hum. Genomics* **2009**, *3*, 362.
4. Penning, T. M.; Burczynski, M. E.; Jez, J. M.; Hung, C. F.; Lin, H. K.; Ma, H.; Moore, M.; Palackal, N.; Ratnam, K. *Biochem. J.* **2000**, *351*, 67.
5. Penning, T. M. *Hum. Reprod. Update* **2003**, *9*, 193.
6. Piekorz, R. P.; Gingras, S.; Hoffmeyer, A.; Ihle, J. N.; Weinstein, Y. *Mol. Endocrinol.* **2005**, *19*, 431.
7. Higaki, Y.; Usami, N.; Shintani, S.; Ishikura, S.; El-Kabbani, O.; Hara, A. *Chem. Biol. Interact.* **2003**, *143–144*, 503.
8. Lambert, J. J.; Belelli, D.; Hill-Venning, C.; Peters, J. A. *Trends Pharmacol. Sci.* **1995**, *16*, 295.
9. Hsu, N. Y.; Ho, H. C.; Chow, K. C.; Lin, T. Y.; Shih, C. S.; Wang, L. S.; Tsai, C. M.; Smuc, T. *Cancer Res.* **2001**, *61*, 2727.
10. Smuc, T.; Hevir, N.; Ribic-Pucelj, M.; Husen, B.; Thole, H.; Rizner, T. L. *Mol. Cell. Endocrinol.* **2009**, *301*, 59.
11. Chen, Y. J.; Yuan, C. C.; Chow, K. C.; Wang, P. H.; Lai, C. R.; Yen, M. S.; Wang, L. S. *Gynecol. Oncol.* **2005**, *97*, 110.
12. Chow, K. C.; Lu, M. P.; Wu, M. T. *J. Dermatol. Sci.* **2006**, *41*, 205.
13. Chien, C. W.; Ho, I. C.; Lee, T. C. *Carcinogenesis* **2009**, *30*, 1813.
14. Deng, H. B.; Adikari, M.; Parekh, H. K.; Simpkins, H. *Cancer Chemother. Pharmacol.* **2004**, *54*, 301.
15. Wang, H. W.; Lin, C. P.; Chiu, J. H.; Chow, K. C.; Kuo, K. T.; Lin, C. S.; Wang, L. S. *Int. J. Cancer* **2007**, *120*, 2019.
16. Selga, E.; Noé, V.; Ciudad, C. *J. Biochem. Pharmacol.* **2008**, *75*, 414.
17. Gobec, S.; Brozic, P.; Rizner, T. L. *Bioorg. Med. Chem. Lett.* **2005**, *15*, 5170.
18. Brozic, P.; Cesar, J.; Kovac, A.; Davies, M.; Johnson, A. P.; Fishwick, C. W.; Lanisnik Rizner, T.; Gobec, S. *Chem. Biol. Interact.* **2009**, *178*, 158.
19. Brozic, P.; Kocbek, P.; Sova, M.; Kristl, J.; Martens, S.; Adamski, J.; Gobec, S.; Lanisnik Rizner, T. *Mol. Cell. Endocrinol.* **2009**, *301*, 229.
20. Dhagat, U.; Carbone, V.; Chung, R. P.; Matsunaga, T.; Endo, S.; Hara, A.; El-Kabbani, O. *Med. Chem.* **2007**, *3*, 546.
21. Dhagat, U.; Endo, S.; Sumii, R.; Hara, A.; El-Kabbani, O. *J. Med. Chem.* **2008**, *51*, 4844.
22. El-Kabbani, O.; Scammells, P. J.; Gosling, J.; Dhagat, U.; Endo, S.; Matsunaga, T.; Soda, M.; Hara, A. *J. Med. Chem.* **2009**, *52*, 3259.
23. El-Kabbani, O.; Scammells, P. J.; Day, T.; Dhagat, U.; Endo, S.; Matsunaga, T.; Soda, M.; Hara, A. *Eur. J. Med. Chem.* **2010**, *45*, 5309.
24. El-Kabbani, O.; Carper, D. A.; McGowan, M. H.; Devedjiev, Y.; Rees-Milton, K. J.; Flynn, T. G. *Proteins* **1997**, *29*, 186.